Molecular Psychiatry (2004) 9, 325

www.nature.com/mp

IMAGE

Functional but not structural subgenual prefrontal cortex abnormalities in melancholia

DA Pizzagalli[1], TR Oakes[2], AS Fox[2], MK Chung[2,3], CL Larson[4], HC Abercrombie[5], SM Schaefer[4], RM Benca[5] and RJ Davidson[2,4,5]

[1]*Department of Psychology, Harvard University, Cambridge, MA, USA;* [2]*W.M. Keck Laboratory for Functional Brain Imaging and Behavior, University of Wisconsin, Madison, WI, USA;* [3]*Department of Statistics, University of Wisconsin, Madison, WI, USA;* [4]*Department of Psychology, University of Wisconsin, Madison, WI, USA;* [5]*Department of Psychiatry, University of Wisconsin, Madison, WI, USA*

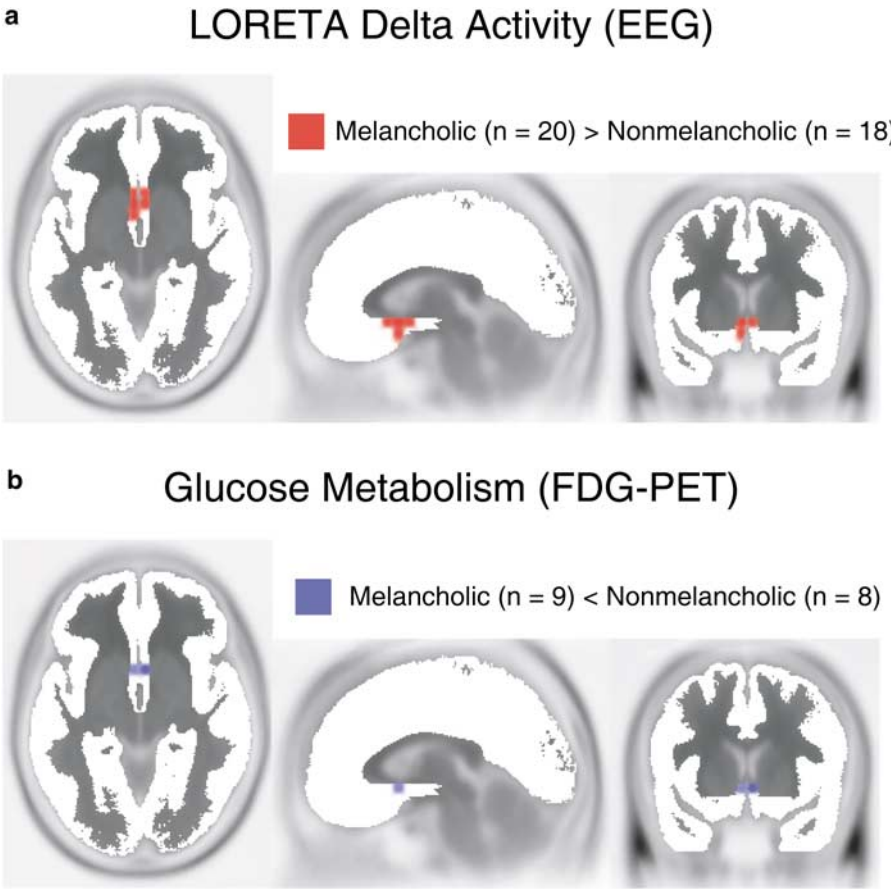

Molecular Psychiatry (2004) **9,** 325. doi:10.1038/sj.mp.4001501

LORETA and FDG-PET whole-brain analyses. Results of voxel-by-voxel *t*-tests contrasting melancholic and nonmelancholic subjects in (a) delta (1.5–6.0 Hz) current density (LORETA), and (b) regional glucose metabolism (FDG-PET). Red: relatively higher delta activity for melancholic subjects. Blue: relatively lower regional glucose metabolism for melancholic subjects. Statistical maps are thresholded at $P < 0.05$ (corrected) and displayed on the MNI template. For more information on this topic, please see the article by Pizzagalli *et al.* on page 393–405.

Molecular Psychiatry (2004) 9, 393–405

www.nature.com/mp

ORIGINAL RESEARCH ARTICLE

Functional but not structural subgenual prefrontal cortex abnormalities in melancholia

DA Pizzagalli[1], TR Oakes[2], AS Fox[2], MK Chung[2,3], CL Larson[4], HC Abercrombie[5], SM Schaefer[4], RM Benca[5] and RJ Davidson[2,4,5]

[1]*Department of Psychology, Harvard University, Cambridge, MA, USA;* [2]*WM Keck Laboratory for Functional Brain Imaging and Behavior, University of Wisconsin, Madison, WI, USA;* [3]*Department of Statistics, University of Wisconsin, Madison, WI, USA;* [4]*Department of Psychology, University of Wisconsin, Madison, WI, USA;* [5]*Department of Psychiatry, University of Wisconsin, Madison, WI, USA*

Major depression is a heterogeneous condition, and the search for neural correlates specific to clinically defined subtypes has been inconclusive. Theoretical considerations implicate frontostriatal, particularly subgenual prefrontal cortex (PFC), dysfunction in the pathophysiology of melancholia—a subtype of depression characterized by anhedonia—but no empirical evidence has been found yet for such a link. To test the hypothesis that melancholic, but not nonmelancholic depression, is associated with the subgenual PFC impairment, concurrent measurement of brain electrical (electroencephalogram, EEG) and metabolic (positron emission tomography, PET) activity were obtained in 38 unmedicated subjects with DSM-IV major depressive disorder (20 melancholic, 18 nonmelancholic subjects), and 18 comparison subjects. EEG data were analyzed with a tomographic source localization method that computed the cortical three-dimensional distribution of current density for standard frequency bands, allowing voxelwise correlations between the EEG and PET data. Voxel-based morphometry analyses of structural magnetic resonance imaging (MRI) data were performed to assess potential structural abnormalities in melancholia. Melancholia was associated with reduced activity in the subgenual PFC (Brodmann area 25), manifested by increased inhibitory delta activity (1.5–6.0 Hz) and decreased glucose metabolism, which themselves were inversely correlated. Following antidepressant treatment, depressed subjects with the largest reductions in depression severity showed the lowest post-treatment subgenual PFC delta activity. Analyses of structural MRI revealed no group differences in the subgenual PFC, but in melancholic subjects, a negative correlation between gray matter density and age emerged. Based on preclinical evidence, we suggest that subgenual PFC dysfunction in melancholia may be associated with blunted hedonic response and exaggerated stress responsiveness.
Molecular Psychiatry (2004) **9**, 393–405. doi:10.1038/sj.mp.4001469
Published online 30 December 2003

Keywords: depression; anhedonia; positron emission tomography; magnetic resonance imaging; voxel-based morphometry; low-resolution electromagnetic tomography (LORETA)

Introduction

To overcome the limitations of a psychiatric nosology restricted to descriptive characteristics, neuroscientific studies in major depressive disorders (MDD) have aimed at defining phenotypes that might be characterized by reliable neural abnormalities.[1,2] Melancholia—a subtype of MDD characterized by pervasive anhedonia and psychomotor disturbances[3,4]—has been hypothesized to involve frontostriatal dysfunctions.[5,6] Accordingly, anhedonia and psychomotor disturbances could be linked to dysfunctions in mesolimbic dopaminergic projections to the ventral medial prefrontal cortex (PFC), ventral anterior cingulate (ACC) and ventral striatum, a network known to implement a 'reward-related system'.[7]

In positron emission tomography (PET) studies of patients with early-onset familial depression with recurrent episodes, decreased activity has been observed in ACC areas located ventral to the genu of the corpus callosum, the so-called subgenual PFC.[8] This finding may be partially accounted for by volumetric reduction[8,9] and morphological changes[10] in this region[11,12] (see Bremner *et al*[11] and Brambilla *et al*[12] for recent failures to replicate volume reductions in the subgenual PFC). Functional and structural abnormalities in the subgenual PFC are intriguing in light of the observation that this region receives one of the richest dopaminergic innervations of any cortical area, particularly from the ventral tegmental area

Correspondence: DA Pizzagalli, Department of Psychology, Harvard University, 1220 William James Hall, 33 Kirkland Street, Cambridge, MA 02138, USA.
E-mail: dap@wjh.harvard.edu
Received 06 July 2003; revised 08 October 2003; accepted 19 November 2003

(VTA),[13] and is known to be implicated in hedonic responsiveness.[7] Consequently, subgenual PFC hypoactivity may impair reward processing. Indeed, based on their findings of decreased activity in the subgenual PFC in familial pure depression,[8] Drevets *et al*[14] hypothesized that the failure of the subgenual PFC to maintain tonic dopaminergic-dependent, reward-related activity may be associated with anhedonia and apathy, two core symptoms of melancholia.

The present investigation tested the hypothesis that melancholic, but not nonmelancholic depression, is specifically associated with reduced activity in the subgenual PFC, a hypothesis that, to the best of our knowledge, has not yet been tested. To this end, simultaneous recording of brain electrical activity (electroencephalogram, EEG) and glucose metabolism (PET) was performed in three subject groups, melancholic and nonmelancholic depressed subjects as well as healthy comparison subjects. To test directly for subtype-specific abnormalities, melancholic and nonmelancholic depressed subjects were contrasted to each other as well as to healthy comparison subjects. EEG data were analyzed with a tomographic source localization technique based on realistic head geometry and probabilistic brain atlases that allowed voxelwise comparisons of brain electrical and metabolic data. To investigate putative structural abnormalities in regions characterized by dysfunctional activity in the EEG/PET data, voxel-based morphometrical analyses of structural magnetic resonance imaging (MRI) data were performed.

Materials and methods

Subjects

Participants were recruited from the community through advertisements in local media (for more detailed information, see Pizzagalli *et al*[15]). The depressed subjects fulfilled DSM-IV criteria for MDD,[16] as determined by the Structured Clinical Interview (SCID) for DSM-IIIR,[17] modified to make DSM-IV diagnoses. These unipolar depressed subjects were further classified as melancholic ($n=20$) or nonmelancholic ($n=18$) based on the presence of DSM-IV melancholic features, and the vast majority of them had experienced several prior depressive episodes. Depressed subjects did not currently meet the criteria for any other Axis I disorders, with exceptions for specific phobias and social phobia secondary to MDD (four melancholic subjects and one nonmelancholic subject had a current specific or social phobia). Dysthymia was permitted if concurrent with MDD (if a subject met the criteria for depression, dysthymia was not further assessed). Familial depression was ascertained in 19 (12 melancholic, seven nonmelancholic) subjects. The exclusion criteria included any history of mania or psychosis in themselves or in first-degree relatives, or current substance abuse (past substance abuse was allowed in the depressed but not the comparison subjects). In the depressed sample, subjects had to be free of alcohol and other substance dependence for at least 6 months. Among the melancholic subjects, two had past alcohol and substance dependence, one reported past alcohol dependence, and one substance dependence. Among the nonmelancholic subjects, two reported past alcohol dependence, one alcohol abuse, one alcohol dependence and substance abuse, and three only substance abuse. Past or present history of Axis II disorders was not assessed. Diagnoses were confirmed by an experienced psychiatrist.

Comparison subjects ($n=18$) were screened using the SCID, Non-patient Edition, and had no history of Axis I pathology. All participants were right-handed, and depressed subjects were free of antidepressant medication for at least 4 weeks prior to recordings. Depressed subjects who participated in the study were free of medication for 2 months or longer. Comparison, melancholic and nonmelancholic subjects did not differ in age (mean: 38.1 years, SD: 13.6; 36.5 ± 12.9; 33.1 ± 8.8), female/male ratio (10/8, 13/7, 10/8), and education[18] (2.3 ± 1.1; 2.6 ± 0.8; 2.9 ± 1.0; possible range: 1 (graduate/professional training) to 7 (less than 7 years of school)). A smaller subsample ($n=29$) underwent concurrent EEG and [^{18}F]-2-fluoro-2-deoxy-D-glucose (FDG) PET recordings, whereas a different subsample of 30 subjects underwent a second EEG recording after the depressed subjects were pharmacologically treated with nortriptyline. Finally, 48 subjects had reliable MRI data that could be used for voxel-based morphometrical analyses. Table 1 summarizes the numbers of subjects per group who were considered for the different subanalyses.

Procedure

At separate sessions, the Hamilton Rating Scale for Depression[19] (HRSD), the SCID, and the Beck Depression Inventory[20] (BDI) were administered after obtaining written informed consent. On a different day, participants underwent concurrent FDG-PET and EEG recording, based on a protocol approved by the

Table 1 Number of subjects included in the different subanalyses

Number of subjects with	*Comparison subjects (N)*	*Melancholic subjects (N)*	*Nonmelancholic subjects (N)*
Reliable EEG data	18	20	18
Reliable EEG and PET data	12	9	8
Reliable EEG data at Times 1 and 2	15	9	6
Reliable MRI data	18	13	17

University of Wisconsin Human Subject Committee. At this session, scalp electrodes (EEG) were first applied, and two intravenous lines were inserted (PET), one for injection, and one for blood draw. EEG was recorded simultaneously with FDG injection and uptake (target FDG dose: 5 mCi; range: 3.8–5.7 mCi), and consisted of 10 contiguous 3-min trials covering the 30 min required for the majority of the radiotracer uptake. Before each trial, subjects were told to open or close their eyes according to a counterbalanced order. A second session with identical procedures took place 4–6 months later and followed pharmacological treatment of the depressed subjects with nortriptyline. Nortriptyline doses were titrated to achieve therapeutic blood levels (50–150 ng/ml). Structural MRI scans were acquired between the pre- (Time 1) and post-treatment (Time 2) session.

Data acquisition

EEG data EEG was recorded from 28 scalp sites referenced to the left ear using a modified lycra electrode cap (Electro-Cap International, Inc.), as previously described in detail.[15]

PET data PET data were acquired using a GE/Advance PET scanner with a 15-cm field of view.[21] Subjects fasted for 5 h prior to the injection of FDG. Arteriolized blood samples were drawn from the left hand for 30 min following injection. After a 10-min break, the subject was positioned on the PET scanner bed (PET scan started approximately 50 min after injection). A 30-min two-dimensional (2D) emission scan, a 10-min three-dimensional (3D) emission scan (not used in the present analyses), and a 10-min transmission scan were acquired.

Structural MRI data A 1.5 T GE Signa scanner (Milwaukee, WI, USA) was used for structural MRI. The MRI protocol consisted of an axial 3D SPGR with the following acquisition parameters: FOV = 24 cm, TE = 14 ms, TR = 30 ms, matrix = 256 × 192, NEX = 1, flip angle = 35°, slice thickness = 1.2 mm, and number of slices = 124.

Data reduction and analyses

EEG data Artifact-free 2048-ms EEG epochs rederived to the average reference were extracted for each trial. For the main analyses, only EEG epochs during eyes-closed trials were used to minimize artifacts caused by eye movements and blinks that may affect low-frequency EEG activity (on average, 140.6 ± 78.4 epochs were available). Spectral analyses were first performed for the 2048-ms epochs using a discrete Fourier transform and boxcar windowing;[22] then, LORETA[23,24] was used to estimate the 3D intracerebral current density distribution for the following bands: delta (1.5–6.0 Hz), theta (6.5–8.0 Hz), alpha1 (8.5–10.0 Hz), alpha2 (10.5–12.0 Hz), beta1 (12.5–18.0 Hz), beta2 (18.5–21.0 Hz), and beta3 (21.5–30.0 Hz). To solve the inverse problem, LORETA assumes that the neighboring neuronal sources are similarly active (ie have similar orientations and strengths), an assumption that is implemented by computing the 'smoothest' of all possible activity distributions (for a summary of recent crossmodal validity, including consistency between LORETA findings and MRI, functional MRI, and electrocorticography from subdural electrodes, see Pizzagalli *et al*[25]).

In the most recent implementation,[24] LORETA employs a three-shell spherical head model[26] and EEG electrode coordinates derived from crossregistrations between spherical and realistic head geometry;[27] the head model and the electrode coordinates were registered to a template MRI from the Brain Imaging Centre, Montreal Neurologic Institute (MNI305[28,29]). The solution space (2394 voxels) achieves a spatial resolution of 7 mm and is restricted to cortical gray matter (GM) and hippocampi, as defined by the digitized MNI probability atlases (ie coordinates reported in the present study are in MNI space). To label gyri and Brodmann area(s) (BA(s)), the Structure–Probability Maps atlas was subsequently used.[30] Since the MNI (used by LORETA) and the Talairach (used by the Structure–Probability Maps atlas) templates do not precisely match, MNI coordinates were converted to Talairach coordinates[31] using the corrections proposed by Brett *et al*[32] (see also http://www.mrc-cbu.cam.ac.uk/Imaging/mnispace.html). At each voxel, LORETA values represent the power, that is, squared magnitude of the computed intracerebral current density (unit: amperes per square meter, A/m^2). For each subject and band, LORETA values were normalized to a total power of 1 and then log transformed before statistical analyses.

PET data Pretreatment 2D PET data were reconstructed using the scanner manufacture's software with calculated attenuation correction to $1.75 \times 1.75 \times 4.25\,mm^3$ voxels, and converted to parametric images of an influx constant (K_i, 1/s) according to a variation of the Sokoloff method[33] (unit: μg/min/100 cc). Blood curves were used to convert the data from units of 'concentration of radioactivity' to 'influx rate constant'. To provide a tracer concentration time course, individual blood time courses measured over the first 30 min were combined with previous normative data collected in our laboratory, yielding a population–average blood curve. Using SPM99,[34] PET data were spatially normalized to the same template as the one used by LORETA (MNI305), converted to $2 \times 2 \times 2\,mm^2$ voxels upon reslicing, and smoothed with a $6 \times 6 \times 6\,mm^2$ Gaussian kernel to approximate the expected resolution of LORETA ($\sim 10\,mm^3$). Using in-house software, the PET data were resampled to yield voxels with the same size and center location as the LORETA voxels. For this step, weighting factors were used, derived by the fractional volume of a PET voxel that was completely or partially within a given LORETA voxel. To match the LORETA solution space, voxels

not considered by LORETA were excluded from the resampled PET data.[35] Finally, PET data were normalized by computing the average value across voxels, and then scaling each image volume so its mean was the same as the mean of all of the individual means (grand mean normalization).

Structural MRI data

Voxel-based morphometry analyses[36] were used to assess possible structural abnormalities in regions showing subtype-specific EEG/PET abnormalities. To this end, T1*-weighted anatomical images were segmented into GM, white matter (WM), and cerebral spinal fluid (CSF) using an automated tissue classification algorithm available in SPM99 (Wellcome Department of Cognitive Neurology, London, UK). This algorithm is based on voxel intensities and uses a combination of prior probability maps and a modified mixture model cluster analysis technique involving a correction for image intensity nonuniformity associated with MRI images.[36] A brain-mask image was created for each subject by applying SPM99's brain extraction algorithm to the original images. A brain-mask template was created by normalizing the original images to a standardized stereotactic space (152-MNI, T1-weighted template from SPM99). This normalization procedure consists of: (a) determining an optimum 12-parameter affine transformation from a given image to the template; and (b) performing a nonlinear estimation of deformations using $4 \times 5 \times 4$ basis functions and little homogeneity correction.[36,37] The deformations acquired by normalizing the original images to the template were applied to the brain-mask images. SPM99's mean function was used to average the brain-mask images together and create a study-specific brain-mask template. To match the hard-coded 8 mm smoothing applied to the input images in SPM99's spatial normalization algorithms, the brain-mask template was blurred using an 8 mm FWHM Gaussian smoothing kernel. The brain-mask images were then normalized to the brain-mask template, and the resulting deformations were applied to the original images. These images were then segmented to produce normalized probability maps of GM, WM, and CSF. Finally, the normalized GM and WM images were cleaned up by dividing the probabilities of each segment by the combined probability that each voxel is part of the GM, WM, or CSF probability images, while nonbrain tissue was masked using SPM99's brain extraction algorithm.

Statistical analyses

For the self-report measures, unpaired *t*-tests were used for assessing group differences. To identify putative subtype-specific functional abnormalities, for both the EEG and PET data, melancholic and nonmelancholic subjects were directly contrasted on a voxelwise basis using unpaired *t*-tests implemented in the LORETA software package. A randomization procedure was implemented to control for Type I errors arising from multiple comparisons.[15] When considering melancholic and nonmelancholic subjects, the false-positive rate estimated after 5000 iterations and averaged across bands was $t_{36} = 2.54$ (two-tailed $P < 0.05$, corrected). The PET data were thresholded at the same statistical level, corresponding to $t_{15} = 2.73$. Brain region(s), BA(s), and Talairach coordinates closest to significant results were determined using the Structure–Probability Maps atlas.[30]

For the voxel-based morphometrical data, a region-of-interest (ROI) approach was used to test whether regions showing subtype-specific functional abnormalities would also show structural abnormalities. To this end, two-way analyses of covariance (ANCOVAs) were run separately on GM and WM probability values extracted from clusters identified in the EEG/PET analyses. *Group* (comparison subjects: $n = 18$; melancholics: $n = 13$; nonmelancholics: $n = 17$) and *Gender* were entered as between-subject factors and *Age* as a covariate. To extract the GM and WM probability values from the only ROI showing subtype-specific abnormalities (ie the subgenual PFC), the following approach was used. An initial mask was created by setting the indices for the six LORETA voxels of interest in a 2394-long LORETA file to 1, with the remaining indices having a value of 0. This mask was subsequently converted to a 3D LORETA file (voxel dimension: 7 mm^3) using an in-house program. This 3D array was then coregistered into MNI space, with the same voxel size (0.859 mm^3) and dimensions (bounding box) as the segmented GM and WM probability maps. During the coregistration process, the data were interpolated, leading to a 'fuzzy' boundary that was no longer composed only of 0's and 1's, but rather of a continuum from 0.0 to 1.0. A threshold of 0.5 was selected, and all values above this threshold were included in the final binary mask, which contained simply 0's outside of the ROI and 1's inside it. An ROI value was obtained for each subject's GM and WM probability maps by extracting the data from each probability map corresponding to the binary mask values with a value of 1, and calculating a mean value.

Results

Self-report measures

Melancholic and nonmelancholic subjects did not differ in their total BDI (33.8 ± 6.4 *vs* 29.5 ± 8.1; $t_{32} = 1.68$, $P > 0.10$) or HRSD (18.2 ± 5.1 *vs* 20.1 ± 5.5; $t_{30} = 1.02$, $P > 0.30$) score.

To test for group differences on specific symptom clusters, BDI scores were aggregated into previously published dimensions derived from principal component analyses,[38] since the present sample size prevented performing factor analyses. The factors were (Table 2): 'negative cognition' (Cronbach alpha: 0.89), 'psychomotor–anhedonia' (alpha: 0.84), 'vegetative symptoms' (alpha: 0.59), and 'somatic symptoms' (alpha: 0.32); due to insufficient reliability index, the vegetative and somatic factors should be inter-

preted with caution. Group differences emerged only for the 'psychomotor–anhedonia' factor, with higher scores for melancholic subjects ($P<0.05$; all other P's >0.24). In an alternative approach, a total 'melancholic' symptom score was computed using BDI items that mapped onto the DSM-IV criteria for melancholia (Cronbach alpha: 0.78): guilty feelings (item #5), agitation (item #11), loss of pleasure/interest (item #12), late insomnia (item #16), and loss of interest in sex (item #21). Consistent with the diagnostic criteria, melancholic subjects endorsed these items more than nonmelancholic subjects (8.88 ± 1.63 *vs* 7.11 ± 2.00; $t_{32}=2.80$, $P<0.009$).

Whole-brain LORETA analyses

Among the seven EEG bands tested with voxelwise unpaired *t*-tests, only delta (1.5–6.0 Hz) and alpha1 (8.5–10.0 Hz) showed significant results ($P<0.05$, corrected) when comparing melancholic and nonmelancholic subjects (Table 3). Compared to nonmelancholic ($n=18$), melancholic subjects ($n=20$) showed relatively higher delta activity ($+16.9\%$; Cohen's effect size[39]: 1) in the subgenual PFC (BA 25) (Figure 1a). Nonmelancholic subjects had higher delta activity than melancholic subjects in a region encompassing the posterior cingulate (BAs 23, 31), precuneus (BAs 7, 31), and paracentral lobule (BAs 5, 6) (Table 3).

For alpha1, melancholic subjects displayed relatively higher activity in a small cluster in the left parietal lobe (Table 3), whereas nonmelancholic subjects showed relatively higher alpha1 activity in a large right-hemispheric cluster that included the inferior (BAs 11, 45, 47) and middle (BAs 10, 11, 46) frontal gyri, the inferior (BA 20), middle (BA 21), and superior (BAs 13, 22, 38, 41, 42) temporal gyri, as well as the precentral (BAs 6, 44) and postcentral gyri (BAs 40, 43).

ANCOVA analyses

To test the specificity of these results, two-way ANCOVA with *Group* (comparison, melancholic, nonmelancholic subjects) and *Gender* as between-subject factors and *Age* as covariate were computed. (Age was used as a covariate as ACC activity has been shown to decrease with age.[40]) For each ANCOVA, the averaged LORETA activity extracted from the corresponding cluster was the dependent variable (the ANCOVA assumption of homogeneity of regression slopes was tested by assessing whether interactions between independent variables and the covariate were significant). For all four clusters, the only significant effect to emerge was *Group* (all

Table 2 Mean (and SD) score on BDI factors (according to Dunn *et al*[35]) for melancholic and nonmelancholic subjects

	Melancholic	*Nonmelancholic*	*t values*
Negative cognition	1.70 ± 0.47	1.47 ± 0.61	1.19
Psychomotor–anhedonia	1.74 ± 0.26	1.51 ± 0.32	2.23[a]
Vegetative symptoms	1.46 ± 0.75	1.14 ± 0.74	1.23
Somatic symptoms	0.59 ± 0.58	0.68 ± 0.64	−0.39

Negative cognition: Failure (BDI item #3); self-hate (item #7); punishment (item #6); self-blame (item #8); feels ugly (item #14); guilt (item #5). *Psychomotor–anhedonia*: Loss of pleasure/interest (item #12); agitation (item #11); push to work (item #15); decision difficulty (item #13); anhedonia (item #4). *Vegetative symptoms*: Appetite decrease (item #18); late insomnia (item #16). *Somatic symptoms*: Health worries (item #20); weight decrease (item #19).
[a]$P<0.05$ (unpaired *t*-test): Melancholic subjects differ from nonmelancholic subjects.

Table 3 Summary of significant results emerging from whole-brain LORETA analyses contrasting melancholic ($n=20$) and nonmelancholic ($n=18$) subjects

	X	*Y*	*Z*	*Side*	*Region*	*BA*	*Voxel*	*t value*
Melancholic > nonmel.								
Delta (1.5–6.0 Hz)	−3	10	−6	Bilateral	Subgenual PFC	25	6	2.68
Alpha1 (8.5–10.0 Hz)	−45	−67	22	Left	Middle temporal gyrus	39	2	2.57
Melancholic < nonmel.								
Delta (1.5–6.0 Hz)	−3	−39	50	Bilateral	Precuneus	7	74	–3.01
Alpha1 (8.5–10.0 Hz)	60	−11	8	Right	Superior temporal gyrus	22	229	–2.89

For the delta and alpha1 band, the coordinates, anatomical regions, and BAs of extreme *t* values are listed. Positive *t* values are indicative of stronger current density for melancholic ($n=20$) than nonmelancholic ($n=18$) subjects, and *vice versa* for negative *t* values. The number of voxels exceeding the statistical threshold determined by the randomization procedure is also reported ($P<0.05$, corrected). Coordinates in mm (MNI space), origin at anterior commissure; (X) = left(−) to right(+); (Y) = posterior(−) to anterior(+); (Z) = inferior(−) to superior(+).

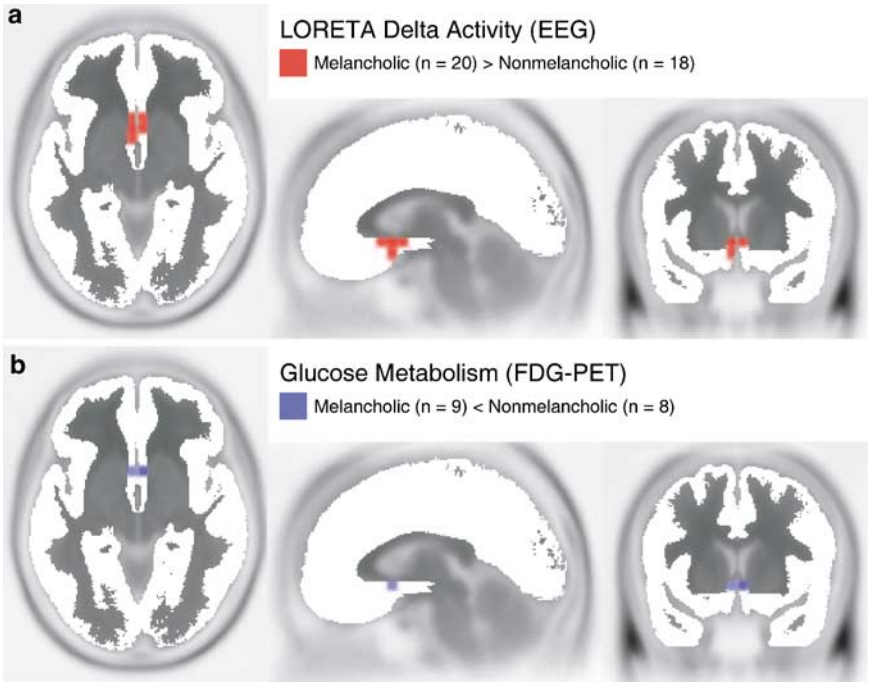

Figure 1 LORETA and FDG-PET whole-brain analyses. Results of voxel-by-voxel *t*-tests contrasting melancholic and nonmelancholic subjects in (a) delta (1.5–6.0 Hz) current density (LORETA) and (b) regional glucose metabolism (FDG-PET). Red: relatively higher delta activity for melancholic subjects. Blue: relatively lower regional glucose metabolism for melancholic subjects. Statistical maps are thresholded at $P<0.05$ (corrected) and displayed on the MNI template.

$F_{2,49}>3.68$, all P's <0.035). For the subgenual PFC, *post hoc* tests (Scheffe) showed that melancholic subjects (adjusted mean: -4.46 ± 0.073) had more delta activity than *both* comparison ($n=18$) (-4.52 ± 0.098; $P<0.045$) and nonmelancholic (-4.52 ± 0.066; $P<0.025$) subjects, with no differences between the latter groups ($P>0.95$). Overall, 18 of the 20 melancholic (binomial $P(18/20)<0.0005$) but only 10 of the 18 nonmelancholic (binomial $P(10/18)$, NS) subjects had more delta activity in the subgenual PFC than the mean of the comparison subjects (Fisher's exact probability <0.020).

For the remaining three clusters, no significant differences emerged between comparison and melancholic subjects, or comparison and nonmelancholic subjects (all P's >0.25). In light of these results and because the main goal of this study was to identify functional abnormalities that would specifically characterize a given depression subtype, further analyses focused on the subgenual PFC cluster only.

Correlations with self-report measures

No significant correlations emerged between any measures of depression severity and pretreatment delta activity in the subgenual PFC for melancholic, nonmelancholic, or all depressed subjects.

FDG-PET data

Figure 1b shows the results of the whole-brain analysis contrasting regional glucose metabolism between melancholic ($n=9$) and nonmelancholic ($n=8$) subjects at the level where maximal differences between the two depressed groups were found in the delta band. The map has been thresholded at the same statistical level as for the LORETA data, which corresponded to $t_{15}=2.73$. Compared to nonmelancholic, melancholic subjects had lower glucose metabolism (–16.4%; Cohen's effect size:[39] 1.33) in voxels that overlapped with the subgenual PFC cluster emerging from the LORETA analyses (Figure 1a). Melancholic and comparison ($n=12$) subjects, however, did not show significantly different activity in the subgenual PFC cluster ($t_{19}=-0.40$; $P>0.60$).

Significant differences between the depressed groups were also found in other regions (not shown). Melancholic subjects showed more glucose metabolism in the right middle frontal (BAs 46, 9, 6), bilateral inferior parietal (BAs 40), left superior temporal (BAs 22, 42), and left postcentral (BA 2) gyri, and less metabolism in the left middle frontal (BA 6), right inferior, and middle temporal (BA 37) gyri, and at the border between the right posterior (BA 23) and anterior (BA 24) cingulate gyri. Due to the limited extent of the regions involved and the small sample size, these PET results should be regarded as preliminary. Nevertheless, it is noteworthy that the subgenual PFC finding overlapped for the two modalities (Figure 1).

Correlation between LORETA and FDG-PET data

To make the PET and LORETA data as comparable as possible, LORETA solutions were recomputed using epochs derived from both the eyes-open and eyes-closed trials, and normalized using the identical

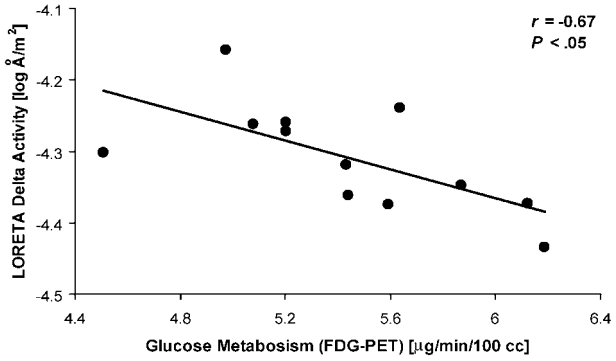

Figure 2 Relation between LORETA delta current density and FDG-PET data. Scatterplot and Pearson's correlations between delta activity (unit: A/m²) and glucose metabolism (unit: μg/min/100 cc) in the subgenual PFC for comparison subjects ($n=18$). For the ordinate, less negative values (log A/m²) reflect higher delta (ie less activity).

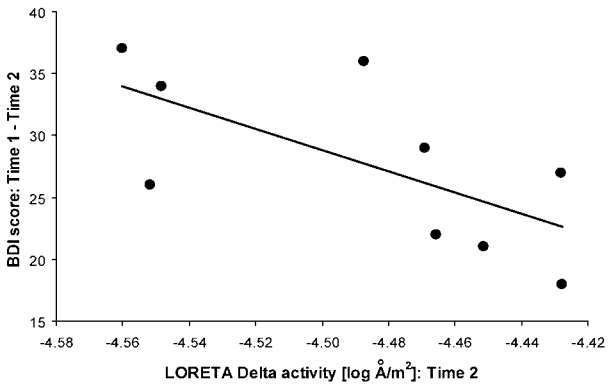

Figure 3 Relation between post-treatment LORETA delta current density and change in depression severity. Scatterplot and Pearson's correlations between delta activity in the subgenual PFC after remission and changes in BDI score (pre- minus post-treatment) for melancholic subjects ($n=20$). For the abscissa, less negative values (log A/m²) reflect higher delta (ie less activity). Time 1: pretreatment, Time 2: post-treatment.

procedure used for the PET data (only 29 subjects had both PET and EEG data). For both modalities, activity was extracted from the subgenual PFC cluster emerging from the LORETA analyses. Significant negative (Pearson) correlations between delta activity and metabolism were found for comparison ($r_{10}=-0.66$, $P<0.030$; Figure 2) but not depressed ($r_{15}=-0.15$, NS) subjects. These correlations were not significantly different ($z=1.49$, $P>0.13$).

Change in LORETA activity after remission

For comparison subjects ($n=15$), the average delta current density in the subgenual PFC at Time 1 (pretreatment for the depressed subjects) and Time 2 (post-treatment) were virtually identical (-4.52 ± 0.10 *vs* -4.52 ± 0.05, $t_{14}=-0.03$, $P>0.95$). Although the two sessions were separated by 4–6 months, delta current density extracted from the subgenual PFC for Times 1 and 2 were moderately correlated ($r=0.48$, one-tailed $P=0.037$).

At the second session, all depressed subjects were remitted, as defined by at least 50% change in BDI score (range: 72.3–100%). For melancholic ($t_8=2.04$, $P=0.076$; $n=9$) but not nonmelancholic ($t_5=-1.28$, $P>0.25$; $n=6$) subjects, post-treatment delta activity (-4.49 ± 0.05) in the subgenual PFC tended to be lower than pretreatment delta activity (-4.45 ± 0.06) in the same cluster. At post-treatment, melancholic subjects did not differ anymore from either comparison or nonmelancholic subjects in subgenual PFC delta activity (both P's >0.13). On an individual level, seven of the nine melancholic subjects (77.75%) but only two of the six nonmelancholic subjects (33%) showed a decrease from pre- to post-treatment delta activity in BA25 (test for two independent proportions; $z=1.72$, one-tailed $P<0.05$).

For the entire depressed sample, post-treatment delta activity in the subgenual PFC was negatively associated with BDI changes ($r_{13}=-0.71$, $P<0.005$), with a similar pattern for melancholic ($r_7=-0.67$, $P<0.05$; Figure 3) and nonmelancholic ($r_4=-0.67$, $P=0.15$) subjects. Thus, subjects with the lowest level of delta activity after remission showed the largest changes in BDI score (pre- minus post-treatment). For PET data, these analyses were not possible due to the low number of subjects with reliable pre- and post-treatment PET data.

Structural MRI data

Neither for comparison nor depressed subjects, nor for the entire sample, were GM and WM probabilities in the subgenual PFC significantly correlated with delta current density or glucose metabolism extracted from the same cluster (all P's >0.13).

The two-way ANCOVAs with *Group* and *Gender* as between-subject factors and *Age* as covariate revealed no significant results involving *Group* for either the GM ($F_{2,39}=0.83$, $P>0.30$) or WM ($F_{2,39}=0.17$, $P>0.50$) probability values extracted from the subgenual PFC cluster. Melancholic (GM: 0.70 ± 0.09, WM: 0.019 ± 0.011; $n=13$), nonmelancholic (GM: 0.72 ± 0.06, WM: 0.020 ± 0.010; $n=17$), and comparison (GM: 0.69 ± 0.07, WM: 0.02 ± 0.019; $n=18$) subjects had very similar values. Interestingly, for melancholic ($r_{11}=-0.60$, $P<0.030$) but not nonmelancholic ($r_{15}=-0.36$, $P>0.15$) or comparison ($r_{16}=0.21$, $P>0.40$) subjects, a significant negative Pearson's correlation was observed between subgenual PFC GM probability values and age (Figure 4). The correlations for melancholic and comparison subjects were significantly different ($z=2.63$, $P<0.01$), with no reliable differences between other pairs of correlations. For WM, no significant correlations emerged with age for melancholic ($r_{11}=-0.30$), nonmelancholic ($r_{15}=-0.08$), or comparison ($r_{16}=-0.14$) subjects (all P's >0.30).

To test whether the increase in delta current density in the subgenual PFC in melancholic subjects was modulated by structural variations in this region, two

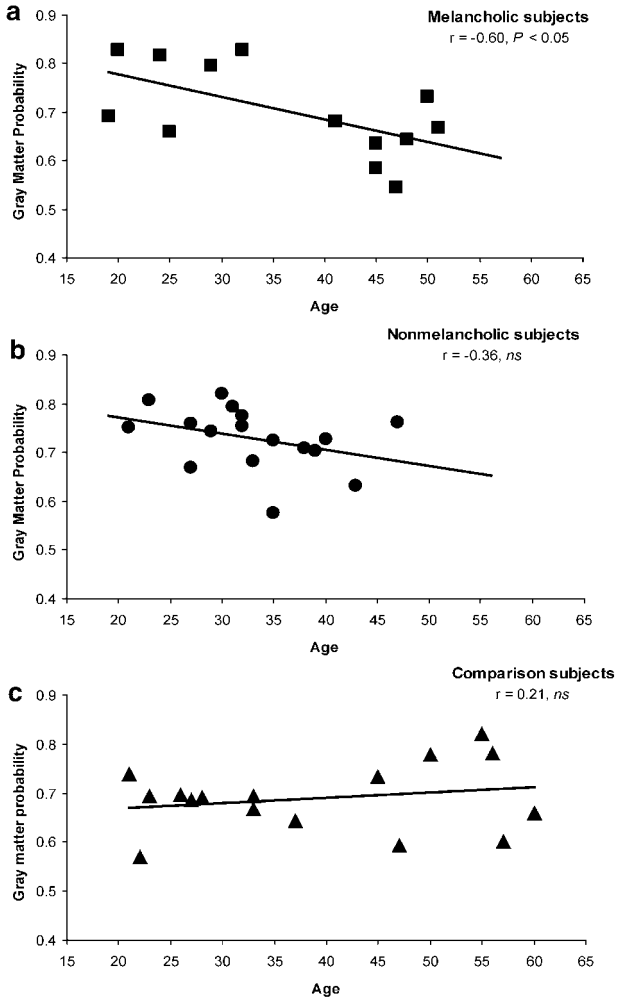

Figure 4 Relations between GM probability and age. Scatterplot and Pearson's correlations between GM probability values and age for (a) melancholic ($n=13$), (b) nonmelancholic ($n=17$), and (c) comparison ($n=18$) subjects.

two-way ANCOVA analyses were run again with *Group* (comparison, melancholic, nonmelancholic subjects) and *Gender* as between-subject factors. In the first ANCOVA, *Age*, *GM probability*, and *WM Probability* were used as covariates; in the second, only *Age* and *GM Probability* served as covariates. Both when including ($F_{2,32}=3.80$, $P<0.035$) or excluding ($F_{2,32}=3.85$, $P<0.035$) *WM Probability* as a covariate, the main effect of *Group* remained significant.

Family history of depression

Owing to reports of subgenual PFC abnormalities in patients with early-onset familial depression,[8,9] additional analyses were run to assess whether findings were further modulated by a family history of depression. Among depressed subjects with EEG data, 19 subjects (11 melancholic and eight nonmelancholic) reported familial depression, and 13 subjects (six melancholic and seven nonmelancholic) denied familial depression. In six subjects, familial depression could not be reliably assessed. Notably, depressed subjects with familial depression were significantly younger than those without familial depression (31.68 ± 10.62 *vs* 40.62 ± 9.25; $t_{30}=2.46$, $P<0.025$). As a result of this age difference, which violated the ANCOVA assumption of homogeneity of regression slopes,[41] hierarchical linear regressions were used instead to evaluate the relations between familial depression, brain measures, and age. Following standard procedures to distinguish shared and nonshared variance among different predictors[42] (pp. 311–320; see also Keller *et al*[41]), age, the interaction between age and familial depression (coded as a dummy variable), and familial depression were sequentially entered to predict brain activity or morphometrical features within the subgenual PFC. For the EEG data (depressed subjects with familial depression: $n=19$, without: $n=13$), PET data (with: $n=10$; without: $n=5$), and GM or WM probabilities (with: $n=16$; without: $n=11$), a family history of depression did not account for additional variance after removing the effects associated with age or the age *x* familial depression interaction (all R^2 change <0.056, all F's <0.90, all P's >0.40).

Control experiment

An independent experiment with five subjects was designed to test whether delta activity in the subgenual PFC may be modulated by eye movements, which can potentially affect activity in lower bands. Delta activity extracted from the subgenual PFC cluster did not differ during eye-closed or eye-open resting, a saccade task, or a smooth pursuit task (Pizzagalli DA *et al*, unpublished observation; results available on request). Delta modulations due to eye movement were found in more caudal and dorsal PFC regions (frontal and supplementary eye field, BA 9/10), as one might expect based on human and animal literature.[43]

Discussion

The aim of the present study was to test the hypothesis that 'dopamine-rich regions of the PFC … are primary sites of dysfunction in melancholia'[6] (p 670). By combining information derived from a distributed inverse solution for EEG data that estimated intracerebral sources of classic frequency bands and FDG-PET, this hypothesis was confirmed. Despite similar levels of depression severity as assessed by two standard measures (BDI and HRSD), melancholic subjects exhibited decreased activity in the subgenual PFC, manifested by relatively stronger delta current density (+16.9%) and lower glucose metabolism (−16.4%) compared to nonmelancholic subjects; according to Cohen[39] the effect sizes observed in the physiological data were large.

Delta activity is considered an inhibitory rhythm, as delta power increases have been observed with brain lesions,[44] anesthesia,[45] and sleep.[46] A recent

study using a modification of LORETA found that sources for delta were in proximity to space-occupying lesions.[47] Further, in patients with Alzheimer's disease[48] and vascular dementia,[49] inverse relationships between scalp-recorded delta activity and glucose metabolism or blood flow have been reported. In the present study, the inverse relationship between delta activity and glucose metabolism in the subgenual PFC strengthens the interpretation of an inhibitory role of delta. Moreover, due to the depth of the region involved, this relationship furnishes important crossmodal validation for the LORETA algorithm. Interestingly, this relationship was not observed in depressed subjects. Since morphological changes in the form of reduced glia cell density have been reported in the subgenual PFC of depressed subjects,[10] and glia cells (particularly, astrocytes) play a critical role in coupling synaptic activity with energy metabolism,[50] the lack of correlation may index a possible decoupling between brain electrical activity and glucose metabolism in depressed individuals. Whereas this decoupling hypothesis should be tested in future studies, we note that initial voxel-based morphometrical analyses based on an ROI approach suggested that dysfunctional subgenual PFC activity in melancholic subjects was not accompanied by structural abnormalities. Independent of relations between the EEG and PET data, the present findings are consistent with prior scalp EEG reports of increased (anterior) slow wave activity in MDD patients with psychomotor retardation (eg Monakhov and Perris[51] and Nieber and Schlegel[52]).

Functional abnormalities in the subgenual PFC are intriguing in light of reports of reduced volume[8,9] and number of glia cells[10] in a slightly more anterior portion of this region of patients with a familial history of depression—a dysfunction that appears early in the manifestation of the illness[9] and does not normalize after remission[8] (see Bremner *et al*[11] and Brambilla *et al*[12], for failures to replicate structural abnormalities in the subgenual PFC). Whether morphometrical abnormalities in the current melancholic sample were present at a finer-graded level of spatial resolution than what could be achieved by voxel-based morphometrical analyses is currently unknown. We note, however, that a tendency for normalization of delta activity (ie decrease in delta or increase in activation) in the subgenual PFC was observed in melancholic subjects after successful pharmacological treatment. Interestingly, for melancholic subjects and more generally for the entire depressed sample, high levels of post-treatment delta activity in the subgenual PFC—indicative of functional hypoactivity—were linked to smaller changes in depression severity. The present morphometrical findings and those from prior studies[8,9,11,12] converge, suggesting unaltered structural features in the subgenual PFC of *non*familial mood disorder patients. However, findings in familial patients are mixed, both positive[8,9] and negative (Brambilla *et al*[12] and present study). These discrepancies may be related to differences in patient samples, particularly in terms of the severity of the disease. Subgenual PFC structural abnormalities have indeed been reported in moderately to severely depressed[8] and hospitalized first-episode[9] patients, but not in less severely depressed and unmedicated outpatients (Brambilla *et al*[12] and the present study).

Although no differences in morphological features were observed among groups, a significant negative correlation between age and GM probability was observed for melancholic, but not nonmelancholic or comparison, subjects. Thus, the older the melancholic subjects, the lower the GM density in the subgenual PFC. Since these findings were not predicted *a priori*, caution should be exerted in interpreting them. We note, however, that recent studies by Parker *et al*[53,54] have shown that age has an important influence on the phenotypic expression of melancholia. More specifically, in melancholic—but not nonmelancholic—depression, psychomotor disturbances increased with age, and the effectiveness of selective serotonin reuptake inhibitors decreased with age, leading the authors to suggest that functional or structural disruptions of frontostriatal pathways may lead to a fuller expression of melancholia.[54] Whether the age-dependent decrease in GM probability in a dopaminergic-rich PFC region observed here represents a biological marker of age-related changes in the phenotypic expression of melancholia is currently unknown. Note also that a third variable associated with age not assessed in the present analyses (eg higher number of depressive episodes, longer exposure to stress) may have mediated this correlation. Consistent with this conjecture, the number of depressive episodes has been recently found to be negatively correlated with normalized glucose metabolism in the subgenual PFC in treatment-resistant unipolar depression;[55] further, long-term exposure to chronic stress and increased sensitization to stress has been associated in preclinical studies with impairment in mesocorticolimbic pathways.[56]

In addition to the delta results involving the subgenual PFC, melancholic and nonmelancholic subjects significantly differed in other regions. Specifically, melancholic subjects showed relatively higher alpha1 current density (ie lower activation) than nonmelancholic subjects in a small cluster in the left parietal lobe. Conversely, nonmelancholic subjects showed relatively higher alpha1 activity in a large right-hemispheric frontotemporal cluster as well as relatively higher delta activity (ie lower activation) in a medial posterior region involving the posterior cingulate, precuneus, and paracentral lobule. Since neither melancholic nor nonmelancholic subjects differed from comparison subjects in these additional regions, these findings should be replicated by future studies and they are not discussed further here.

A paucity of functional neuroimaging studies has specifically investigated patterns of brain activation in melancholia, and the results are inconclusive. In

single-photon emission-computed tomography studies, null findings[57,58] or higher pretreatment rostral ACC activity in melancholic subjects who responded to sleep deprivation than nonresponders[59] have been reported. In PET studies, decreased glucose metabolism in the left dorsolateral PFC[60] and increased blood flow in the left ventrolateral PFC[61] has been observed in melancholic patients. In a recent EEG study based on the same subject sample,[25] we found that both melancholic and nonmelancholic subjects showed relatively increased right PFC and decreased posterior cingulate activity compared to healthy comparison subjects. In melancholic subjects only, however, right prefrontal activity was associated with increased levels of anxiety and depression severity. These findings motivated the present analyses, which focused on direct comparisons of melancholic and nonmelancholic subjects. The results suggest that this approach may be more sensitive for identifying subtype-specific patterns of dysfunctional brain activity. Overall, the present study extended the prior findings by: (a) directly comparing melancholic and nonmelancholic subjects on a voxel-by-voxel basis; (b) investigating the PET data recorded concurrently with the EEG data; (c) investigating the relationships of brain electrical (EEG) and metabolic (PET) activity on a voxel-by-voxel basis; and (d) investigating putative structural abnormalities using voxel-based morphometrical analyses of structural MRIs. From a methodological perspective, the overlap of subgenual PFC clusters implicated in the LORETA and PET analyses and the moderate test–retest reliability of current density from this deep structure for the comparison subjects over a 4- to 6-month period furnish important validation for the LORETA source localization approach.

Before discussing the potential functional implications of the subgenual PFC impairment in melancholia, further functional neuroimaging results in major depression should be emphasized. First, lower subgenual PFC activation was recently observed in depressed subjects with psychotic features compared to depressed subjects without psychotic features and comparison subjects.[62] Interestingly, the authors speculated that the presence of pathological guilt in psychotic depression may mediate the link to dysfunctional subgenual PFC. The fact that guilt is also highly prevalent in melancholic depression would explain the similarity between the current findings and those of Skaf and co-workers. Second, in a recent PET study of unipolar depression, Dunn *et al*[38] reported that a psychomotor–anhedonia symptom cluster defined by principal component analysis of the BDI scale was associated with lower normalized regional glucose metabolism in various right hemispheric regions (including the insula, putamen, dorsolateral PFC, and the extended amygdala), and with higher normalized metabolism in posterior and ACC cortex and medial PFC. These findings contrast with the present results, Drevets *et al*[14] and Skaf *et al*[62] findings, and may be due to methodological differences between the studies, including differences in patients' clinical profile (treatment-resistant depression *vs* community sample) and task (auditory attentional task *vs* resting). Alternatively, some of the items included in the psychomotor–anhedonia factor by Dunn *et al* (eg decreased thought speed and impaired decision making) may not completely map onto the DSM-IV categorical dimension of melancholia. Notably, in a further report by the same group,[55] inverse associations between the subgenual PFC activation and depression severity as well as number of episodes have been reported. Third, whereas Skaf *et al*,[62] Drevets *et al*,[14] and the present study emphasize decreased subgenual PFC activity in the pathophysiology of depression, Mayberg *et al*[63] reported that remission from depression was associated with a *decrease* in subgenual PFC activation, in a cluster (Talairach coordinates: $x=4$, $y=2$, $z=-4$) that was, however, more anterior compared to the one reported in the current study (transformed MNI to Talairach coordinates: $x=-2.97$, $y=9.44$, $z=-5.52$; difference vector: 10.30 mm). Accordingly, either decreased subgenual PFC is present only in specific depression subgroups, including early-onset familial depression with recurrent episodes,[14] psychotic depression,[62] and melancholia (present study), or the subgenual PFC region involved in Mayberg's studies is functionally distinct from the one reported here.

In melancholia, subgenual PFC dysfunction may have deleterious consequences in two domains: exaggerated stress responsiveness and blunted hedonic response. With respect to stress, animal studies have shown that lesions of infralimbic areas that correspond to the primate subgenual PFC led to exaggerated responsiveness of the mesolimbic dopamine system to stress, including increased sympathetic arousal and corticosterone responses,[56,64,65] suggesting that the subgenual PFC plays an inhibitory role in stress-related visceral responses. Although it is unclear whether these data may extend to humans, it is interesting to note that melancholia is associated with sustained hyperactivity of the stress response systems,[66] and that stress plays a critical role in triggering or exacerbating depression.[67] Animal models of 'anhedonia' further suggest that chronic mild stress may subsequently lead to plastic changes in the mesocorticolimbic system, including blunted dopamine response to rewards.[56] These preclinical studies suggest that some subtypes of depression may be linked to deficits in learning and expression of appetitive motivation.[68] Recent reports that early traumatic affective-social experiences—which are often prominent in depression[69]—can alter synaptic and dendritic development in the pregenual ACC[70] further underscore how functional proprieties of the mesolimbic pathways can be shaped during development.

With respect to hedonic responses, the involvement of the ACC in reward monitoring and behavioral adjustment to optimize reward has been demonstrated in monkeys.[71] Electrophysiological studies in

rodents have further demonstrated that neurons in the medial PFC and ventral ACC projecting to the VTA activate the ascending mesocortical dopamine neurons.[72] Recent human neuroimaging studies also highlight a critical role of the subgenual PFC in reward processing and monitoring of behaviorally salient stimuli. The increased activation in the subgenual PFC has been observed in response to sustained reward in a gambling task,[73] unpredictable reward,[74] pleasant somatosensory stimulation,[75] and selective attention to emotional stimuli.[76] In addition, strong appetitive states such as hunger in food-deprived subjects[77] and 'positive feelings' following the administration of an opioid agonist[78] have been linked to ventral ACC activation involving the subgenual PFC. Overall, these findings are consistent with the assumption of reduced reactivity to positive cues in melancholia, one of the core DSM-IV symptoms of this disorder.

Limitations

Although the present findings drawn from three different neuroimaging techniques (EEG, PET, and MRI) highlight a potential role of the subgenual PFC in melancholic depression, it is important to acknowledge some limitations of the present study. First, no neuropsychological or psychomotor measures were collected to differentiate objectively between melancholic and nonmelancholic subjects; although the findings of the self-report measures (BDI scale) confirmed differences in symptom clusters—but not *depression severity*—between these depression subtypes that were consistent with the categorical distinction, more quantitative measures of anhedonia and psychomotor disturbances should be used in future studies. Accordingly, the present findings do not imply that melancholia, as defined by the DSM-IV diagnostic criteria, is neurobiologically homogeneous. Also, without objective and quantitative measures of anhedonia, it is currently unclear whether impaired hedonic capacity in nonmelancholic subjects may be subserved by similar or different neural substrates.

Second, some of the analyses, particularly those involving the PET and the post-treatment data, were limited by a reduced sample size, and thus some of the findings await empirical replication. While one of the main strengths of this study was the integration of various neuroimaging techniques (EEG, PET, and MRI), the complexity of the protocol may have contributed to patients' attrition and data loss.

Third, it is unclear whether the present findings based on a community sample of relatively young, moderately severely depressed patients will extend to different patient samples (eg older inpatients with severe and refractory depression). Particularly, although it is not uncommon to assess community samples or outpatients with melancholic depression[79–83] with a mean age in the mid-30s as in the present sample,[83] the prevalence of melancholia is typically higher in more severely ill and older (in)patients.[79,84–86] Also, although the melancholic subjects met rigorous inclusion criteria, they were able to refrain from medication and to participate in a complex and multimodal study, suggesting that they likely represented a less severe sample than others described in the literature.[87,88]

Finally, although depressed and comparison subjects enrolled in this study did not have any current substance abuse, no data were available for smoking habits/history. Since nicotine may affect hedonic responsiveness in MDD via its action on mesolimbic DA reward system,[89] future neuroimaging studies should assess whether the level of nicotine use has a modulatory role in functional and structural brain abnormalities in MDD and the phenotypic expression of melancholia.

Conclusions

In conclusion, by combining information derived from FDG-PET and a distributed inverse solution for EEG data constrained by a probabilistic brain atlas that estimated intracerebral sources of classic EEG frequency bands, we found that melancholia was specifically associated with decreased activity in the subgenual PFC. This subtype-specific functional abnormality emerged in the absence of structural abnormalities, at least at the spatial resolution afforded by voxel-based morphometrical analyses of MRI images. When considered in the framework of extant preclinical literature, this functional abnormality may represent a possible neural correlate of anhedonia that prominently characterizes this subtype of depression.

Acknowledgements

We thank John Koger for computer assistance and Megan Zuelsdorff, Andrew M Hendrick, Kathryn A Horras, and Allison Jahn for assistance. This work was supported by NIMH Grants (MH40747, P50-MH52354, MH43454) and by an NIMH Research Scientist Award (K05-MH00875) to RJD. DAP was supported by grants from the Swiss National Research Foundation (81ZH-52864) and 'Holderbank'-Stiftung zur Förderung der wissenschaftlichen Fortbildung. CLL was supported by an NRSA Predoctoral Fellowship Award (F31-MH12085).

References

1 Davidson RJ, Pizzagalli D, Nitschke JB, Putnam K. Depression: perspectives from affective neuroscience. *Annu Rev Psychol* 2002; **53**: 545–574.
2 Drevets WC. Neuroimaging and neuropathological studies of depression: implications for the cognitive–emotional features of mood disorders. *Curr Opin Neurobiol* 2001; **11**: 240–249.
3 Parker G, Hadzi-Pavlovic D, Austin MP, Mitchell P, Wilhelm K, Hickie I *et al*. Sub-typing depression, I. Is psychomotor disturbance necessary and sufficient to the definition of melancholia? *Psychol Med* 1995; **25**: 815–823.

4 Rush AJ, Weissenburger JE. Melancholic symptom features and DSM-IV. *Am J Psychiatry* 1994; **151**: 489–498.
5 Rogers MA, Bradshaw JL, Pantelis C, Phillips JG. Frontostriatal deficits in unipolar major depression. *Brain Res Bull* 1998; **47**: 297–310.
6 Austin MP, Mitchell P. The anatomy of melancholia: does frontal–subcortical pathophysiology underpin its psychomotor and cognitive manifestations? *Psychol Med* 1995; **25**: 665–672.
7 Wise RA, Rompre PP. Brain dopamine and reward. *Annu Rev Psychol* 1989; **40**: 191–225.
8 Drevets WC, Price JL, Simpson JRJ, Todd RD, Reich T, Vannier M *et al.* Subgenual prefrontal cortex abnormalities in mood disorders. *Nature* 1997; **386**: 824–827.
9 Hirayasu Y, Shenton ME, Salisbury DF, Kwon JS, Wible CG, Fischer IA *et al.* Subgenual cingulate cortex volume in first-episode psychosis. *Am J Psychiatry* 1999; **156**: 1091–1093.
10 Öngür D, Drevets WC, Price JL. Glial reduction in the subgenual prefrontal cortex in mood disorders. *Proc Natl Acad Sci USA* 1998; **95**: 13290–13295.
11 Bremner JD, Vythilingam M, Vermetten E, Nazeer A, Adil J, Khan S *et al.* Reduced volume of orbitofrontal cortex in major depression. *Biol Psychiatry* 2002; **51**: 273–279.
12 Brambilla P, Nicoletti MA, Harenski K, Sassi RB, Mallinger AG, Frank E *et al.* Anatomical MRI study of subgenual prefrontal cortex in bipolar and unipolar subjects. *Neuropsychopharmacology* 2002; **27**: 792–799.
13 Gaspar P, Berger B, Febvret A, Vigny A, Henry JP. Catecholamine innervation of the human cerebral cortex as revealed by comparative immunohistochemistry of tyrosine hydroxylase and dopamine-beta-hydroxylase. *J Comp Neurol* 1989; **279**: 249–271.
14 Drevets WC, Öngür D, Price JL. Neuroimaging abnormalities in the subgenual prefrontal cortex: implications for the pathophysiology of familial mood disorders. *Mol Psychiatry* 1998; **3**: 220–226.
15 Pizzagalli D, Pascual-Marqui RD, Nitschke JB, Oakes TR, Larson CL, Abercrombie HC *et al.* Anterior cingulate activity as a predictor of degree of treatment response in major depression: evidence from brain electrical tomography analysis. *Am J Psychiatry* 2001; **158**: 405–415.
16 American Psychiatric Association. *Diagnostic and Statistical Manual of Mental Disorders*, 4th edn. American Psychiatric Association: Washington, DC, 1994.
17 Spitzer RL, Williams JBW, Gibbon M, First MB. *Structured Clinical Interview for DSM-III-R*. American Psychiatric Press: Washington, DC, 1992.
18 Hollingshead AB. *Two Factor Index of Social Position*. Yale University: New Haven, CT, 1957.
19 Hamilton M. A rating scale for depression. *J Neurol Neurosurg Psychiatry* 1960; **23**: 56–62.
20 Beck AT, Ward CH, Medleson M, Mock J, Erbaugh J. An inventory for measuring depression. *Arch Gen Psychiatry* 1961; **4**: 561–571.
21 Abercrombie HC, Schaefer SM, Larson CL, Oakes TR, Holden JE, Perlman SB *et al.* Metabolic rate in the right amygdala predicts negative affect in depressed patients. *Neuroreport* 1998; **9**: 3301–3307.
22 Brillinger DR. *Time Data Analysis and Theory*. McGraw-Hill: New York, 1981.
23 Pascual-Marqui RD, Michel CM, Lehmann D. Low resolution electromagnetic tomography: a new method for localizing electrical activity in the brain. *Int J Psychophysiol* 1994; **18**: 49–65.
24 Pascual-Marqui RD, Lehmann D, Koenig T, Kochi K, Merlo MC, Hell D *et al.* Low resolution brain electromagnetic tomography (LORETA) functional imaging in acute, neuroleptic-naive, first-episode, productive schizophrenia. *Psychiatry Res: Neuroimaging* 1999; **90**: 169–179.
25 Pizzagalli DA, Nitschke JB, Pascual-Marqui RD, Larson CL, Abercrombie HC, Schaefer SM *et al.* Brain electrical tomography abnormalities in depression: the importance of melancholic features and anxiety. *Biol Psychiatry* 2002; **52**: 73–85.
26 Ary JP, Klein SA, Fender DH. Location of sources of evoked scalp potentials: corrections for skull and scalp thicknesses. *IEEE Trans Biomed Eng* 1981; **28**: 447–452.
27 Towle VL, Bolanos J, Suarez D, Tan K, Grzeszczuk R, Levin DN *et al.* The spatial location of EEG electrodes: locating the best-fitting sphere relative to cortical anatomy. *Electroencephalogr Clin Neurophysiol* 1993; **86**: 1–6.
28 Evans AC, Collins DL, Mills SR, Brown ED, Kelly RL, Peters TM. 3D statistical neuroanatomical models from 305 MRI volumes. *Proc IEEE Nucl Sci Symp Med Imag Conf* 1993; **95**: 1813–1817.
29 Collins DL, Neelin P, Peters TM, Evans AC. Automatic 3D intersubject registration of MR volumetric data in standardized Talairach space. *J Comput Assist Tomogr* 1994; **18**: 192–205.
30 Lancaster JL, Rainey LH, Summerlin JL, Freitas CS, Fox PT, Evans AC *et al.* Automated labeling of the human brain—a preliminary report on the development and evaluation of a forward-transformed method. *Hum Brain Mapp* 1997; **5**: 238–242.
31 Talairach J, Tournoux P. *Co-planar Stereotaxic Atlas of the Human Brain*. Thieme Medical Publishers, Inc.: New York, 1988.
32 Brett M, Johnsrude IS, Owen AM. The problem of functional localization in the human brain. *Nat Rev Neurosci* 2002; **3**: 243–249.
33 Phelps ME, Huang SC, Hoffman EJ, Selin C, Sokoloff L, Kuhl DE. Tomographic measurement of local cerebral glucose metabolic rate in humans with (F-18)2-fluoro-2-deoxy-D-glucose: validation of method. *Ann Neurol* 1979; **6**: 371–388.
34 Friston KJ, Worsley KJ, Frackowiak RSJ, Mazziotta JC, Evans AC. Assessing the significance of focal activations using their spatial extent. *Hum Brain Mapp* 1994; **1**: 214–220.
35 Oakes TR, Pizzagalli D, Hendrick AM, Horras KA, Larson CL, Abercrombie HC *et al.* Functional coupling of simultaneous electrical and metabolic activity in the human brain. *Hum Brain Mapp*. (in press).
36 Ashburner J, Friston KJ. Voxel-based morphometry—the methods. *Neuroimage* 2000; **11**: 805–821.
37 Ashburner J, Friston KJ. Nonlinear spatial normalization using basis functions. *Hum Brain Mapp* 1999; **7**: 805–821.
38 Dunn RT, Kimbrell TA, Ketter TA, Frye MA, Willis MW, Luckenbaugh DA *et al.* Principal components of the Beck Depression Inventory and regional cerebral metabolism in unipolar and bipolar depression. *Biol Psychiatry* 2002; **51**: 387–399.
39 Cohen J. *Statistical Power Analysis for the Behavioral Sciences*. Erlbaum Associates: Hillsdale, NJ, 1988.
40 Volkow ND, Logan J, Fowler JS, Wang GJ, Gur RC, Wong C *et al.* Association between age-related decline in brain dopamine activity and impairment in frontal and cingulate metabolism. *Am J Psychiatry* 2000; **157**: 75–80.
41 Keller J, Nitschke JB, Bhargava T, Deldin PJ, Gergen JA, Miller GA *et al.* Neuropsychological differentiation of depression and anxiety. *J Abnorm Psychol* 2000; **109**: 3–10.
42 Cohen J, Cohen P. *Applied Multiple Regression/Correlation Analysis for the Behavioral Sciences*. Erlbaum Associates: Hillsdale, NJ, 1983.
43 Tehovnik EJ, Sommer MA, Chou IH, Slocum WM, Schiller PH. Eye fields in the frontal lobes of primates. *Brain Res Brain Res Rev* 2000; **32**: 413–448.
44 Gilmore PC, Brenner RP. Correlation of EEG, computerized tomography, and clinical findings. Study of 100 patients with focal delta activity. *Arch Neurol* 1981; **38**: 371–372.
45 Reddy RV, Moorthy SS, Mattice T, Dierdorf SF, Deitch Jr RD. An electroencephalographic comparison of effects of propofol and methohexital. *Electroencephalogr Clin Neurophysiol* 1992; **83**: 162–168.
46 Niedermeyer E. Sleep and EEG. In: Niedermeyer E, Lopes da Silva F, (eds). *Electroencephalography: Basic Principles, Clinical Applications, and Related Fields*, 3rd edn Williams & Wilkins: Baltimore, MD, 1993 pp. 153–166.
47 Fernandez-Bouzas A, Harmony T, Bosch J, Aubert E, Fernandez T, Valdes P *et al.* Sources of abnormal EEG activity in the presence of brain lesions. *Clin Electroencephalogr* 1999; **30**: 46–52.
48 Valladares-Neto DC, Buchsbaum MS, Evans WJ, Nguyen D, Nguyen P, Siegel BV *et al.* EEG delta, positron emission tomography, and memory deficit in Alzheimer's disease. *Neuropsychobiology* 1995; **31**: 173–181.
49 Szelies B, Mielke R, Kessler J, Heiss WD. EEG power changes are related to regional cerebral glucose metabolism in vascular dementia. *Clin Neurophysiol* 1999; **110**: 615–620.
50 Magistretti PJ. Cellular bases of functional brain imaging: insights from neuron–glia metabolic coupling. *Brain Res* 2000; **886**: 108–112.

51 Monakhov K, Perris C. Neurophysiological correlates of depressive symptomatology. *Neuropsychobiology* 1980; **6**: 268–279.
52 Nieber D, Schlegel S. Relationships between psychomotor retardation and EEG power spectrum in major depression. *Neuropsychobiology* 1992; **25**: 20–23.
53 Parker G. Differential effectiveness of newer and older antidepressants appears mediated by an age effect on the phenotypic expression of depression. *Acta Psychiatr Scand* 2002; **106**: 168–170.
54 Parker G, Roy K, Hadzi-Pavlovic D, Wilhelm K, Mitchell P. The differential impact of age on the phenomenology of melancholia. *Psychol Med* 2001; **31**: 1231–1236.
55 Kimbrell TA, Ketter TA, George MS, Little JT, Benson BE, Willis MW *et al.* Regional cerebral glucose utilization in patients with range of severities of unipolar depression. *Biol Psychiatry* 2002; **51**: 237–252.
56 Cabib S, Puglisi-Allegra S. Stress, depression and the mesolimbic dopamine system. *Psychopharmacology* 1996; **128**: 331–342.
57 Schlegel S, Adenhoff JB, Eissner D, Linder P, Nickel O. Regional cerebral blood flow in depression: associations with psychopathology. *J Affect Disord* 1989; **17**: 211–218.
58 Delvenne V, Delecluse F, Hubain PP, Schoutens A, De Maertelaer V, Mendlewicz J. Regional cerebral blood flow in patients with affective disorders. *Br J Psychiatry* 1990; **157**: 359–365.
59 Ebert D, Feistel H, Barocka A, Kaschka W. Increased limbic blood flow and total sleep deprivation in major depression with melancholia. *Psychiatry Res* 1994; **55**: 101–109.
60 Martinot JL, Hardy P, Feline A, Huret JD, Mazoyer B, Attar-Levy D *et al.* Left frontal glucose hypometabolism in the depressed state: a confirmation. *Am J Psychiatry* 1990; **147**: 1313–1317.
61 Drevets WC, Videen TO, Price JL, Preskorn SH, Carmichael T, Raichle ME. A functional anatomical study of unipolar depression. *J Neurosci* 1992; **12**: 3628–3641.
62 Skaf CR, Yamada A, Garrido GEJ, Buchpiguel CA, Akamine S, Castro CC *et al.* Psychotic symptoms in major depressive disorder are associated with reduced regional cerebral blood flow in the subgenual anterior cingulated cortex: a voxel-based single photon emission computed tomography (SPECT) study. *J Affect Disord* 2002; **68**: 295–305.
63 Mayberg HS, Liotti M, Brannan SK, McGinnis S, Mahurin RK, Jerabek PA *et al.* Reciprocal limbic-cortical function and negative mood: converging PET findings in depression and normal sadness. *Am J Psychiatry* 1999; **156**: 675–682.
64 Deutch AY, Clark WA, Roth RH. Prefrontal cortical dopamine depletion enhances the responsiveness of mesolimbic dopamine neurons to stress. *Brain Res* 1990; **521**: 311–315.
65 Sullivan RM, Gratton A. Lateralized effects of medial prefrontal cortex lesions on neuroendocrine and autonomic stress responses in rats. *J Neurosci* 1999; **19**: 2834–2840.
66 Gold PW, Licinio J, Wong ML, Chrousos GP. Corticotropin releasing hormone in the pathophysiology of melancholic and atypical depression and in the mechanism of action of antidepressant drugs. *Ann NY Acad Sci* 1995; **771**: 716–729.
67 Kendler KS, Kessler RC, Walters EE, MacLean C, Neale MC, Heath AC *et al.* Stressful life events, genetic liability, and onset of an episode of major depression in women. *Am J Psychiatry* 1995; **152**: 833–842.
68 Di Chiara G, Loddo P, Tanda G. Reciprocal changes in prefrontal and limbic dopamine responsiveness to aversive and rewarding stimuli after chronic mild stress: implications for the psychobiology of depression. *Biol Psychiatry* 1999; **46**: 1624–1633.
69 Kaufman J, Plotsky PM, Nemeroff CB, Charney DS. Effects of early adverse experiences on brain structure and function: clinical implications. *Biol Psychiatry* 2000; **48**: 778–790.
70 Helmeke C, Ovtscharoff W, Poeggel G, Braun K. Juvenile emotional experience alters synaptic inputs on pyramidal neurons in the anterior cingulate cortex. *Cereb Cortex* 2001; **11**: 717–727.
71 Shima K, Tanji J. Role for cingulate motor area cells in voluntary movement selection based on reward. *Science* 1998; **282**: 1335–1338.
72 Au-Young SM, Shen H, Yang CR. Medial prefrontal cortical output neurons to the ventral tegmental area (VTA) and their responses to burst-patterned stimulation of the VTA: neuroanatomical and *in vivo* electrophysiological analyses. *Synapse* 1999; **34**: 245–255.
73 Elliott R, Friston KJ, Dolan RJ. Dissociable neural responses in human reward systems. *J Neurosci* 2000; **20**: 6159–6165.
74 Berns GS, McClure SM, Pagnoni G, Montague PR. Predictability modulates human brain response to reward. *J Neurosci* 2001; **21**: 2793–2798.
75 Francis S, Rolls ET, Bowtell R, McGlone F, O'Doherty J, Browning A *et al.* The representation of pleasant touch in the brain and its relationship with taste and olfactory areas. *Neuroreport* 1999; **10**: 453–459.
76 Elliott R, Rubinsztein JS, Sahakian BJ, Dolan RJ. Selective attention to emotional stimuli in a verbal go/no-go task: an fMRI study. *Neuroreport* 2000; **11**: 1739–1744.
77 Tataranni PA, Gautier JF, Chen KW, Uecker A, Bandy D, Salbe AD *et al.* Neuroanatomical correlates of hunger and satiation in humans using positron emission tomography. *Proc Natl Acad Sci USA* 1999; **96**: 4569–4574.
78 Schlaepfer TE, Strain EC, Greenberg BD, Preston KL, Lancaster E, Bigelow GE, Barta PE, Pearlson GD. Site of opioid action in the human brain: mu and kappa agonists' subjective and cerebral blood flow effects. *Am J Psychiatry* 1998; **155**: 470–473.
79 Benazzi F. Psychomotor changes in melancholic and atypical depression: unipolar and bipolar-II subtypes. *Psychiatry Res* 2002; **112**: 211–220.
80 Benedictis E. Double-blind comparison of venlafaxine and amitriptyline in outpatients with major depression with or without melancholia. *J Psychopharmacol* 2000; **14**: 61–66.
81 Heiligenstein JH, Tollefson GD, Faries DE. Response patterns of depressed outpatients with and without melancholia: a double-blind, placebo-controlled trial of fluoxetine *vs* placebo. *J Affect Disord* 1994; **30**: 163–173.
82 Kendler KS. The diagnostic validity of melancholic major depression in a population-based sample of female twins. *Arch Gen Psychiatry* 1997; **54**: 299–304.
83 Türkçapar MH, Akdemir A, Örsel SD, Demirergi N, Sirin A, Kiliç EZ *et al.* The validity of diagnosis of melancholic depression according to different diagnostic systems. *J Affect Disord* 1999; **54**: 101–107.
84 Enns MW, Larsen DK, Cox BJ. Discrepancies between self and observer ratings of depression the relationship to demographic, clinical and personality variables. *J Affect Disord* 2000; **60**: 33–41.
85 Parker G, Roy K, Hadzi-Pavlovic D, Mitchell P, Wilhelm K, Menkes DB *et al.* Sub-typing depression by clinical features: the Australasian DataBase. *Acta Psychiatr Scand* 2000; **101**: 21–28.
86 Parker G, Hadzi-Pavlovic D, Wilhelm K, Hickie I, Brodaty H, Boyce P *et al.* Defining melancholia: properties of a refined sign-based measure. *Br J Psychiatry* 1994; **164**: 316–326.
87 Schotte CK, Maes M, Cluydts R, Cosyns P. Cluster analytic validation of the DSM melancholic depression. The threshold model: integration of quantitative and qualitative distinctions between unipolar depressive subtypes. *Psychiatry Res* 1997; **71**: 181–195.
88 Guelfi JD, Ansseau M, Timmerman L, Kørsgaard S, Mirtazapine-Venlafaxine Study Group. Mirtazapine *vs* venlafaxine in hospitalized severely depressed patients with melancholic features. *J Clin Psychopharmacol* 2001; **21**: 425–431.
89 Quattrocki E, Baird A, Yurgelun-Todd D. Biological aspects of the link between smoking and depression. *Harv Rev Psychiatry* 2000; **8**: 99–110.